Proceedings of the 2007 IEEE/RSJ International
Conference on Intelligent Robots and Systems
San Diego, CA, USA, Oct 29 - Nov 2, 2007

Over-the-Horizon, Autonomous Navigation for Planetary Exploration

Ioannis Rekleitis, Jean-Luc Bedwani, and Erick Dupuis
Canadian Space Agency, Space Technologies
6767 route de l'aéroport, Saint-Hubert (Québec), J3Y 8Y9, Canada
FirstName.LastName@space.gc.ca

Abstract— **The success of NASA's Mars Exploration Rovers has demonstrated the important benefits that mobility adds to planetary exploration. Very soon, mission requirements will impose that planetary exploration rovers drive over-the-horizon in a single command cycle. This will require an evolution of the methods and technologies currently used. This paper presents experimental validation of our over-the-horizon autonomous planetary navigation. We present our approach to 3D terrain reconstruction from large sparse range data sets, localization and autonomous navigation in a Mars-like terrain. Our approach is based on on-line acquisition of range scans, map construction from these scans, path planning and navigation using the map. An Autonomy Engine supervises the whole process ensuring the safe navigation of the planetary rover. The outdoor experimental results demonstrate the effectiveness of the reconstructed terrain model for rover localization, path planning and motion execution scenario as well as the autonomy capability of our approach.**

I. INTRODUCTION

The recent success of the Mars Exploration Rovers "Spirit" and "Opportunity" has demonstrated the important benefits that mobility adds to landed planetary exploration missions [1]. The recent announcement by NASA to increase its activities in planetary exploration (via Moon and Mars missions) and the ESA Aurora program will certainly result in an increase in the number of robotic vehicles roaming on the surface of other planets. In particular, robotics will play a critical role in NASA's Mars Science Laboratory [2] and ESA's Exo-Mars [3], [4]. The current state-of-the-art in control of planetary rovers requires intensive human involvement throughout the planning portion of the operations. Unless the terrain is relatively easy to navigate, rovers are typically limited to traverses on the order of a few tens of meters. Recently, the Mars Exploration Rovers "Spirit" and "Opportunity" have managed to conduct traverses on the order of 100 meters per day.

To increase the science return, future planetary missions will undoubtedly require the ability to traverse even longer distances. Given the long communication delays and narrow communication windows of opportunity, it is impossible for Earth-based operators to drive Mars rovers in an interactive manner. Furthermore, over long traverses, the detailed geometry of the environment cannot be known a-priori. In this context, planetary rovers will require the ability to navigate autonomously over long distances.

So far very little is implemented in terms of autonomous decision-making capability. Operations are based on pre-planned, pre-verified command scripts. When situations requiring some sort of decision are encountered, the robot must usually stop and wait for a human operator to intervene. For example, in the case of the rovers "Spirit" and "Opportunity", once an interesting geological feature has been identified, it takes at least two command cycles (of 12 hours each) to go apply an instrument to it [5]. The scientific return on investment is therefore severely limited by the limited on-board autonomy capability.

Fig. 1. The Mars terrain with our modified P2AT.

The next rover missions to Mars are the "Mars Science Laboratory" (MSL) [6] and ESA's ExoMars [4]. Both of these missions have set target traverse distances on the order of one kilometre per day. Both the MSL and ExoMars rovers are therefore expected to drive regularly a significant distance beyond the horizon of their environment sensors. Earth-based operators will therefore not know a-priori the detailed geometry of the environment and will thus not be able to select via points for the rovers throughout their traverses. Path and trajectory planning will have to be conducted on-board, which is an evolution from the autonomy model of the MERs.

One of the key technologies that will be required is the ability to sense and model the 3D environment in which the rover has to navigate. The current sensing model is based on passive vision. We are currently developing the capabilities of active vision systems such as 3D laser range finders. For long-range navigation, the ability to localize the rover through the registration of sensor data with the model of the 3D terrain is also required. To address these issues, we are developing a suite of technologies for long-range rover navigation. For the purposes of this paper, "long-range" is defined as a traverse that takes the rover beyond the horizon of the rover's environment sensors.

The typical operational scenario used for our experimentation is based on the following assumptions. The rover, see

1-4244-0912-8/07/$25.00 ©2007 IEEE.

Fig. 1, has rough a-priori knowledge of its surroundings in the form of a low-resolution terrain map. The interaction between the rover and the Earth-based operator is limited to a single command specifying a target destination in absolute coordinates. The rover must first observe its environment to localize itself accurately. It then plans a rough path in the coarse terrain model that will take it from its current estimated position to the target destination. After obtaining this rough path, the rover iteratively takes local scans of its surroundings and navigates segments of the planned path. The local scans are used for three purposes: planning a local path to the next way-point while avoiding known obstacles, refining the localization knowledge throughout the trajectory by observing again the traversed terrain, and finally constructing an atlas [7], [8] of detailed terrain maps to be added to the coarse terrain model.

Key to our terrain modelling is the Irregular Triangular Mesh (ITM) [9] representation of the sensor data. ITM was selected because it preserves the accuracy of sensor data, can be easily used for path/task planning, and allow for compact and memory efficient storage without significant loss of precision.

This paper presents the key components that have been developed in our laboratory to address the above mentioned critical issues in rover navigation. The latest experimental results that have been obtained are also presented. The next Section presents the related work, while Section III outlines the over-the-horizon navigation process. The terrain modelling algorithms and experimental results obtained on CSA's Mars emulation terrain (Mars terrain) are in Section IV. Section V provides an overview of the localization scheme along with qualitative experimental results. Path-planning and Navigation are outlined in Section VI. Experimental results for the integrated rover navigation experiments are provided in Section VII. Finally, the last Section contains concluding remarks and future work.

II. Background

Over the years different researchers have proposed a variety of schemes for planetary exploration addressing a variety of problems [10]. Terrain mapping was proposed to assist a walking robot as early as 1994 [11]. The main sensor proposed in the literature has been a vision system, either monocular [12] or stereo [13].

In the area of path-planning, a bug-like algorithm was proposed for micro-rovers [14], while potential-field like methods were also suggested [15]. The autonomy aspects of planetary exploration have been discussed ranging from trajectory planning in simulation [16] to varying behaviours based on the vision sensor data collected [17] and for ensuring visual coverage [18]. Finally the problem of human to rover interactions has also been studied [19], [20].

Currently, the most advanced exploration robots for planetary exploration are the Mars Exploration Rovers (MER) "Spirit" and "Opportunity". These rovers have successfully demonstrated, on Mars, concepts such as visual odometry and autonomous path selection from a terrain model acquired from sensor data [1]. The main sensor suite used for terrain assessment for the MER has been passive stereo vision [21]. The models obtained through stereo imagery are used both for automatic terrain assessment and for visual odometry.

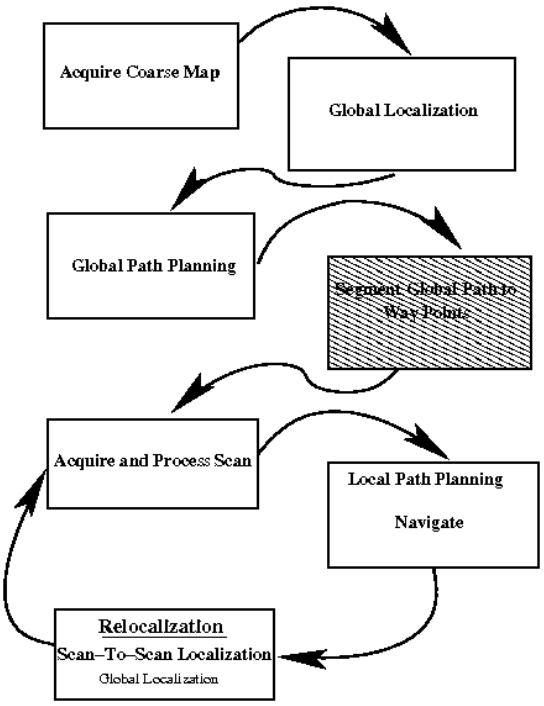

Fig. 2. The overall process.

In the case of automatic terrain assessment, the cloud of 3D points is used to evaluate the traversability of the terrain immediately in front of the rover, defined as a regular grid of square patches. In the case of visual odometry, the model is used to identify and track features of the terrain to mitigate the effect of slip. [22]

Our work focuses on a different sensing modality, a laser range finder which returns accurate geometric information in three dimensions. One interesting feature of such sensors is that they already provides three-dimensional data in the form of a 3D point cloud. In addition, since they do not rely on ambient lighting, we do not have to address the problems arising from adverse lighting conditions. We are taking advantage of this sensor characteristic to build a terrain model that preserves the geometry of the terrain but that is also readily usable for path planning and navigation.

III. Over-the-Horizon Navigation

The overall process used to conduct the over-the-horizon navigation experiments is illustrated by Fig. 2. In this figure, the boxes represent discrete steps to be executed by the robot throughout the traverse and arrows represent transitions between the discrete steps. The transitions are typically triggered by external events or by the completion of the previous steps. Note that only the nominal scenario is depicted in Fig. 2: a robust fully autonomous state machine would include many more steps and transitions.

The process starts with the acquisition of a coarse map of the area from a library of terrain maps. The robot then uses the scanning LIDAR to obtain a series of terrain scans to be used to localize the robot as precisely as possible on the coarse map. A coarse model of the terrain is then generated

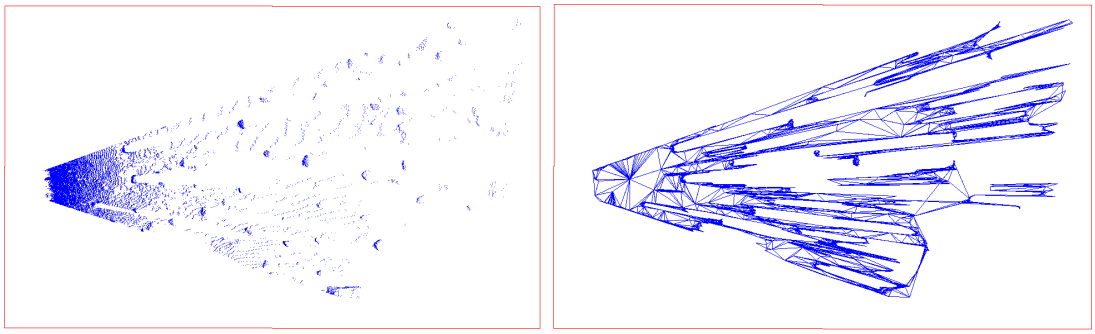

(a) (b)

Fig. 3. (a) A LIDAR scan; (b) the same scan decimated and represented as a triangular mesh.

in the irregular triangular mesh format and is used to plan a path from the robot's current position (found through global localization) to the operator-entered destination.

The path is then segmented into a sequence of way-points that are consistent with the robot's mobility and the range of the scanning LIDAR. After the robot has obtained a coarse segmented path, it iteratively performs a sequence of local traverses by acquiring detailed environment scans along the next path segment, building a local model of the terrain, planning a path through it and moving towards the next way-point in the coarse path. At the end of every local traverse, the rover turns around and acquires a scan of the terrain looking back towards the previous location. This scan is used to reset the drift in odometry by performing scan-to-scan localization between terrain models obtained in consecutive scans. It is worth noting that the resolution of the global map is usually coarse enough that it makes it unsuited for correcting the odometric drift between successive scans. It can be used though, every few scans in order to further constraint the inevitable drift. During our experiments we never applied this method.

In the next sections we are going to discuss in more details some of the necessary steps.

IV. Terrain Modelling

The first step in the navigation process is the sensing and modelling of the terrain through which the rover will navigate. The terrain sensor used on CSA's experimental test-bed is a commercial LIght Detection And Ranging (LIDAR) sensor: an ILRIS-3D sensor from Optech. The main advantage of the LIDAR is that it directly provides a 2.5D point cloud giving the x-y-z coordinates of the terrain in its field of view. The sensor has a range of over 1 kilometre but because of the size of the experimental terrain, the sensor is set to return data-points up to approximately 30 metres away. Some of the specific challenges that must be addressed by the terrain modelling software are the high volume of data (each LIDAR scan can contain as many as 500K 3D points), and the highly non-uniform density of the scans which is due to the fact that the sensor is mounted at a grazing angle. Indeed, to increase the challenges associated with over-the-horizon navigation, the sensor is mounted directly on top of the rover (approximately 50 cm off the ground; see Fig. 1). This has the effect of shortening the horizon and introducing severe occlusions in the presence of obstacles; see Fig. 3a.

Since a point cloud is not an appropriate structure for path-planning and navigation, a different representation has to be chosen. One of the requirements of the selected representation is that it must be compatible with navigation algorithms and that it must preserve the scientific data contained in the terrain topography. In addition, the resulting model must be compact in terms of memory usage since the model must reside on-board the rover. To fulfil these requirements, the Irregular Triangular Mesh (ITM) terrain representation was chosen.

The first step to build the mesh is to connect the neighbouring points in the point cloud. The meshing is performed using Delaunay triangulation [23] and realising that the point cloud from any single scan always forms a 2.5D representation because the LIDAR can only observe what is in its direct line-of-sight. The next step is then to remove triangles that have been formed in the shadows behind the objects in the field of view (thus called shadow triangles). It is worth noting that the operation of removing these triangles often results to several disconnected components of the ITM, which is an acceptable result. The implementation of the terrain modelling using a triangular mesh is done using the Visualisation Toolkit [24] libraries.

One of the main advantages of the ITM over the classical digital elevation maps (DEM) is that it inherently supports variable resolution. It is therefore possible to decimate the data set, modelling details of uneven areas with high precision, while simplifying flat areas to just a few triangles; see Fig. 3b for a decimated triangular mesh of the data points presented in Fig. 3a. The decimated mesh drastically reduces the overall memory requirements for a given terrain.

The majority of previous work on 3D mapping is centered on creating models for urban environments or man-made artifacts. Much of the existing research on 3D mapping using LIDAR sensors has used sweeping line sensors [25], [26], [27]. However, some work using 3D scanning LIDAR has also been published [28], [29]. The other popular sensing modality is stereo vision [30], [31], which typically works at shorter range but has the advantage of providing photo-realistic models at no cost. Please note, that most of the above mentioned approaches show little or no concern about using the resulting mesh for navigation.

The ITM representation also has advantages compared to other variable resolution representations such as quad-

		Target Decimation Ratio							
	Orig. Scans	75%		80%		90%		95%	
		Number	Real %	Number	Real %	Number	Real %	Number	Real %
Points (mean)	31248	8077	74.06%	6532	79%	3439	88.86%	2088	93.09%
Points (std)	7840		0.70%		0.74%		1.16%		2.31%
Triangles(mean)	61670	15417	75.00%	12333	80.00%	6194	89.91%	3591	94.01%
Triangles(std)	15787		0.00%		0.00%		0.75%		1.90%

TABLE I

PROPERTIES OF DECIMATED TERRAIN SCANS, ACCEPTABLE ERROR 1.5CM

trees or other traversability maps, which remove all science content from the topographical data. In addition, both DEM and quad-trees are 2.5D representations. Therefore, they do not support concave geological structures like overhangs and caverns, which pose no problem to the irregular triangular mesh. Recently, a new approach has been proposed that combines a DEM with multiple layers [32] thus allowing for the modelling of overhangs but it still suffers from memory and traversability issues.

The terrain decimation algorithms were run over all LIDAR scans (91 scans) acquired during the 2006 field-testing season[1]. Four different decimation targets were set for the algorithm (70%, 80%, 90% and 95%). The algorithm attempts to reduce the number of triangles in the model to match the decimation target (for a 70% target ratio, the algorithm keeps 30% of the triangles). The error threshold sets an upper limit on the decimation ratio by ensuring that the error between the decimated mesh and the original mesh does not exceed a set value. The error is defined as the Euclidean distance between the original point cloud and the triangular cells composing the decimated mesh (point-to-surface distance). A maximum error threshold was set at 1.5 cm. The error threshold was selected to ensure that the terrain decimation would not flatten obstacles that are beyond the obstacle traversing capability of the CSA's Mobile Robotics Test-bed (MRT). The algorithm stops as soon as the mesh cannot be decimated without violating this threshold.

Our approach uses vtk's DecimatePro mesh decimation algorithms, which remove superfluous triangles in a mesh. The co-planarity of neighbouring triangles is assessed by measuring the dihedral angle through their common edge. A smoothing of the point mesh is performed prior to decimation to account for the fact that the ILRIS 3D LIDAR sensor used for the acquisition of the point cloud has a fixed range accuracy regardless of the measurement range. Thus at very short range, the measurement noise induces large dihedral angles between cells. An important side effect of the terrain-smoothing algorithm is that it introduces significant artefacts in the mesh in the presence of outliers in the point cloud. To avoid the introduction of these artefacts, it is important to reject outliers. This was done by removing points that generate triangles in the mesh with extremely long edges, or that are further away from all their neighbours than a threshold distance.

Table I provides a summary of the results of the terrain decimation on a set of ninety one LIDAR scans. The table indicates the number of points and the number of triangles in the mesh for the original scan and for four different target decimation ratios. It is interesting to note that for most cases, the algorithm was capable of fully achieving the decimation ratio. For both the 70% and 80% targets, the ratios were successfully achieved for all terrain scans including for very rugged and broken terrain. For a target of 90% reduction, the average effective reduction ratio was 89.91% with a standard deviation of 0.75%. In fact, only four scans out of ninety one failed to achieve the 90% target decimation ratio. Finally, for a target decimation ratio of 95%, the effective average ratio over all scans was 94.01% with a standard deviation of 1.90%. Approximately 50% of the scans were successfully decimated to 95%. This indicates that these scans could have been further decimated within the limits imposed by the 1.5cm bounds on error.

[1]CSA's location allows outside testing only during the summer and early fall months, thus, the 2006 testing season was from June to early November.

V. LOCALIZATION

During navigation the rover uses wheel odometry, Inertial Measurement Unit (IMU 300CC-100 from Crossbow technology) readings, and absolute heading data from a digital compass (TCM2 from ActivMedia Robotics) to keep track of its pose. The data from the different sources are fused together using a extended Kalman filter (EKF). The compass is activated only when the robot stops (e.g. for taking a new scan) because the compass data is not reliable when the robot motors are running due to the electromagnetic interference. In Mars exploration, a sun sensor could replace the compass. The angular velocities measured by the IMU are integrated to form the orientation in SO(3) using the quaternion formulation. When the rover stops to collect range data, the IMU and compass components revert to recalibration mode in order to correct data drifting. In particular, the gravitational vector is used to correct the pitch and roll and the absolute heading sensor TMC2 is used to perform the yaw correction. As reported previously [33] the EKF was able to keep the error at 1% of the distance travelled for many cases. Similar work was reported in [34].

The above described EKF is used to provide incremental estimates of the rover's pose starting from an arbitrary pose. However, during planetary exploration it is crucial to estimate the starting pose of the rover in some global frame of reference, a process known as global localization. Furthermore, as the rover travels over long distances the EKF continues to accumulate positional error. In order to reduce the EKF error after the rover has travelled through a scanned area, it rotates and scans back over that same area and registers the two scans. A process we call scan-to-scan localization. Using the scans for localization in 2D has been done extensively [35], [36]. More recently, 3D laser scans have been proposed for localization [37] and 3D SLAM [38]

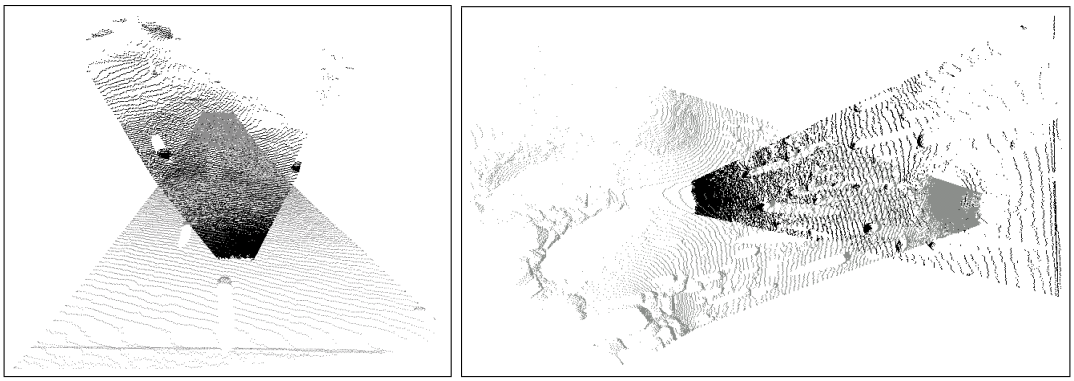

(a) (b)

Fig. 4. Four scans matched pairwise. The first two demonstrate matching using sparse features and the second two using the overall morphology of the environment.

Next we are going to briefly outline these two processes, global and scan-to-scan localization.

A. Global Localization

For global localization, it is assumed that the rover has a-priori knowledge about its immediate environment in the form of a coarse 3D terrain model. Such a model can be provided from satellite imagery, from data collected during landing, or from previous missions. The algorithm must then match the 3D environment model acquired from the rover's point of view with the coarse model. The main difficulties with this operation reside in the fact that the two 3D models are at different resolutions and are taken from different angles.

Two sets of algorithms have been investigated to conduct localization. The first solution uses the Harmonic Shape Image [39] and Spin Image [40] algorithms in tandem, whereas, the second solution uses the point fingerprints method [41]. Preliminary results have been presented previously [42], [43] and further discussion is outside the scope of this paper.

B. Scan to Scan Localization

As mentioned earlier, the purpose of scan-to-scan localization algorithms is to estimate the displacement between successive detailed terrain scans obtained by the rover sensor during navigation. This allows the rover to correctly estimate its current pose compared to the pose from where the previous scan was taken, thus re-calibrating the odometric estimate to cancel IMU drift. This knowledge also allows the mapping algorithm to stitch together detailed terrain maps to obtain a more complete 3D model of the environment. Currently we are employing an implementation of the classical Iterative Closest Point (ICP) algorithm [44]. Please note, that for successful localization using ICP, the error between the two scans has to be small. In particular, the ICP algorithm is run twice, first on the full data of each scan, thus matching the majority of the points that belong to smooth terrain; then the ICP is run a second time on the decimated scans, which results into matching mainly high concentrations of points which represent areas with obstacles. In scan-to-scan localization, the two scans have to be partially overlapping. It is worth noting that the scans have large discrepancies in resolution since they are taken from different points of view and they also have different occluded areas depending on the geometry of the terrain. In particular, due to the low grazing angle at which the sensor is mounted, obstacles (rocks) in the field of view cast long shadows (see Fig. 3a); when an obstacle is viewed from two opposite directions the two opposite faces are recorded with long shadows extending "behind" them, making the matching more challenging.

Figure 4 presents characteristic scan-to-scan matches where the two scans are taken one across from the other. In Fig. 4a, there is only one common rock inside the field of view and the majority of the information was from the slope of the ground. In Fig. 4b, there were many common features it is worth noting the long shadows on the opposite sides of the rocks. Both matches, though not perfect, improved the accuracy of the robot's pose.

VI. Path-Planning and Navigation

Central to the over-the-horizon navigation is the ability to plan and follow a path from the current pose to a pose beyond the sensing horizon. We are using a path-planer based on the adjacency graph of the ITM. The same path-planner is used to acquire a path over the coarse map and then to acquire local paths inside each detailed scan.

At the core of the path-planner is the Dijkstra shortest-path algorithm for weighted graphs. The graph used, as mentioned earlier, is the adjacency graph of the ITM, where the center of each triangle corresponds to a graph-vertex and for two triangles sharing an edge, the corresponding graph-vertices are joined with a graph-edge. From an arbitrary position the planner selects the closest triangle, and then calculates the least expensive path to the triangle closest to the destination. The cost function takes into consideration several parameters: the Euclidean distance between adjacent cells, the terrain slope, and the roughness of the terrain. The slope and roughness are calculated taking into account the rover footprint defined as a circle of given radius. A penalty is added to the Euclidean distance cost when travelling uphill, and threshold values are assigned for uphill, downhill, and cross-track slopes. Beyond these threshold values, the cost of travelling between cells is infinite. The roughness is calculated by taking the dot product of the normal of every pair of adjacent cells in the footprint. The cost is adjusted as a function of this surface roughness parameter to favour

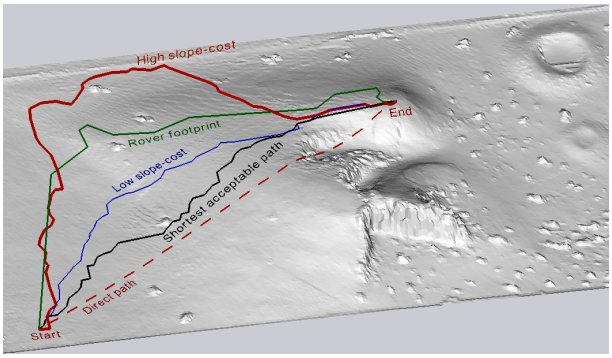

Fig. 5. The model of the Mars terrain and several global paths planned using different cost functions.

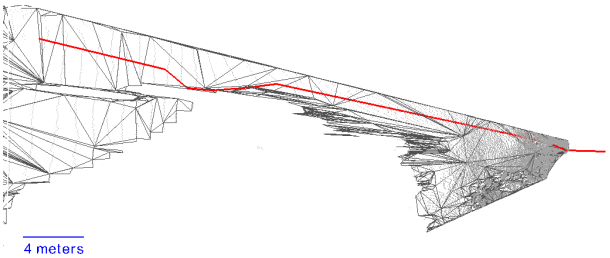

Fig. 6. A scan at the top left side of the Mars terrain, the decimated mesh, and a planned path.

flat surfaces. A threshold value on roughness is also used to assign infinite cost to terrain deemed too rough.

Figure 5 demonstrates the effect of different cost functions on the planned path. The paths were planned using the coarse model of the Mars terrain. The dashed (red) line shows the direct path from start to end without any concern about the slope or the roughness of the terrain. For the rest of the paths only acceptable triangles were considered, that is, triangles with an absolute slope of less than 35 degrees. The (green) line labeled "Rover footprint" plans a path taking into account the rover footprint avoiding high-slope areas and showing a slight preference for flatter terrain. Finally, three paths are planned without taking into account the rovers footprint. The shortest acceptable path planned (black line) is close to the direct path while avoiding the cliff due to the infinite cost of high slope triangles. The second path (blue line) is planned with low slope-cost for acceptable slopes, and the third path (red line) weights flat terrain much higher than distance travelled, thus travelling around the terrain over the most flat areas.

The trajectory generation algorithm produces a trajectory made of straight-line segments joining the centre points of a number of cells in the path. It starts with the list of all cell centre points in the path and removes unnecessary via-points. The algorithm removes intermediate via-points while ensuring that the resulting trajectory still remains strictly on the set of cells that were deemed safe by the path planner. Figure 6 presents a long path planned using a local scan. Due to the low-grazing angle of the LIDAR, the side of the hill in the Mars terrain obstructed a large part of the scan, the path-planner selected triangles that go around the obstruction and at the same time avoid various obstacles.

A low-level motion controller based on a discontinuous state feedback control law, initially proposed by Astolfi [45], is used to guide the rover along the selected way-points. Rigorous experimental results in the Mars terrain have demonstrated the robustness and the stability of the developed path-following approach [46].

VII. Over-the-Horizon Integrated Navigation Experiments

Using the above-described building blocks, a series of "over-the-horizon" traverse experiments were conducted to assess the viability of the proposed concept through field-testing in a realistic environment. In particular, four long-range over-the-horizon traverses were successfully executed. The longest traverse was a loop more than 150m long.

The experiments were run in the Canadian Space Agency's Mars terrain: a 60 meter by 30 meter rover test area that emulates the topography of a broad variety of Martian landscapes. The terrain includes plains, a hill, a canyon and rock fields of varying density. The tests were conducted using our modified Pioneer P2-AT robot (see Fig. 1).

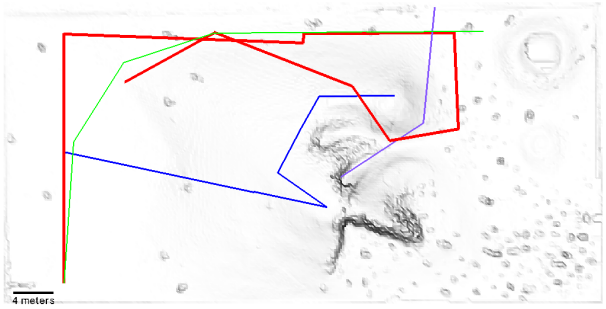

Fig. 7. CSA's Mars-terrain, with the outline of the four successful trajectories.

The experiments described in this paper validated only a portion of the process described on Fig. 2. Indeed, the over-the-horizon traverses were executed in a semi-autonomous manner. Although the global localization has been tested successfully on a limited set of terrain models, it was not ready on time to be included in the experiments. Similarly, the coarse path segmentation was not utilised. The experiments were executed as a sequence of autonomous local traverses where the operator picked a destination point in the field of view of the scanning LIDAR.

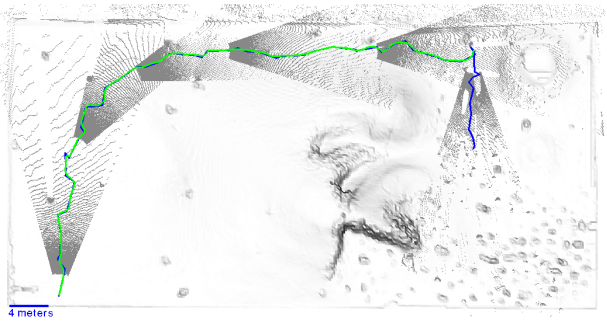

Fig. 8. Successful over-the-horizon navigation.

Four long-range over-the-horizon traverses were successfully executed in this set of experiments. Figure 7 presents

an outline of the four trajectories, as polygonal-lines of the way-points, over a model of the Mars-terrain. In each case, the destination point was not visible to the robot at the beginning of the experiment. Figure 8 presents a six-step trajectory where the rover travelled around the hill. The planned path together with the actual odometric readings are plotted together with the raw LIDAR data. The coarse model of the Mars terrain is also presented in the background as a reference. The longest traverse is illustrated on Fig. 9. Each of the images in Fig. 9 shows the ITM terrain models built from the 3D point clouds acquired by the scanning LIDAR. The bounding box represents the limits of the CSA's Mars terrain. Fig. 9 (a) to (d) show the robot driving around the hill. Fig. 9 (e) to (g) show the robot entering the canyon and climbing on the hill and Fig. 9 (h) to (i) show the robot driving back down the hill towards its final destination. It is interesting to note that in several cases, the horizon of the sensor was extremely short due to the topography of the terrain (Fig. 9 (e) and (f)) thus the planned path was very short. Please note that breaks in the trajectory represent places where high odometry error forced relocalization.

VIII. CONCLUSIONS AND FUTURE WORKS

In this paper we presented the main components required for the successful accomplishment of autonomous planetary exploration. Terrain modelling is a fundamental issue, we propose the irregular triangular mesh as a compact representation that maintains the topography of the terrain. The size reduction via decimation, and the utilization of the mesh in localization, path-planning and navigation have been successfully validated. The ability of a planetary rover to localize accurately in a coarse global map and also after a traverse over a previously mapped terrain is central for the success of future missions. We have developed several techniques for global and scan-to-scan localization. Furthermore, we presented a safe navigation approach using an irregular triangular-mesh terrain representation of the environment which was repeatedly validated in a variety of paths. Several of the building blocks were validated while we also identified weaknesses in the localization approach. Experimental results from traverses each one in excess of 100m were presented.

The advantages of active vision for space applications as demonstrated by the successful use of Neptecs [2] Laser Camera System (LCS) sensor on mission (STS-105) and in every other space shuttle mission since then, are numerous. Moreover, LIDAR sensors from OPTECH [3] have been successfully used in XSS11 rendezvous and docking mission and are part of the future NASA Mars Phoenix mission. LIDAR data are raw 3D points which are available without the cost of image processing, thus eliminating delays and possible errors. In planetary exploration in particular, such a sensor provides accurate data independent of the lighting conditions and allows for multiple uses, such as, accurate mapping of a variety of geological formations, use as a science instrument when combined with techniques such as LASER breakdown spectroscopy, and hazard avoidance during entry, descent, and landing. We are confident that the technologies presented in this paper are going to contribute greatly towards the success of future missions.

[2]http://www.neptec.com

[3]http://www.optech.ca/

REFERENCES

[1] J. Biesiadecki, C. Leger, and M. Maimone, "Tradeoffs between directed and autonomous on the mars exploration rovers," in *Procs. of Int. Symposium of Robotics Research*, San Francisco, 2005.

[2] S. Hayati, G. Udomkesmalee, and R. Caffrey, "Initiating the 2002 mars science laboratory (msl) focused technology program," in *IEEE Aerospace Conf.*, Golden, CO, USA, March 2004.

[3] M. Van Winnendael, B. Gardini, R. Roumeas, and J. Vago, "The exomars mission of esa's aurora programme," in *Earth and Space 2004 - Ninth Biennial Conf. of the Aerospace Division*, Houston, Texas, USA, March 2004.

[4] J. Vago, "Overview of exomars mission preparation," in *8th ESA Workshop on Advanced Space Technologies for Robotics & Automation*, Noordwijk, The Netherlands, November 2004.

[5] L. Pedersen, R. Sargent, M. Bualat, C. Kunz, L. S., and A. Wright, "Single-cycle instrument deployment for mars rovers," in *Procs. of 7th Int. Symposium on Artificial Intelligence, Robotics & Automation in Space*, Nara, Japan, May 2003.

[6] R. Volpe, "Rover functional autonomy development for the mars mobile science laboratory," in *IEEE Aerospace Conf.*, Big Sky, MT, USA, 2006.

[7] M. Bosse, P. Newman, J. Leonard, and S. Teller, "Simultaneous localization and map building in large-scale cyclic environments using the atlas framework," *Int. Journal of Robotics Research*, vol. 23, no. 12, pp. 1113–1139, December 2004.

[8] B. Lisien, D. Morales, D. Silver, G. Kantor, I. M. Rekleitis, and H. Choset, "The hierarchical atlas," *IEEE Trans. on Robotics*, vol. 21, no. 3, pp. 473–481, June 2005.

[9] R. J. Fowler and J. J. Little, "Automatic extraction of irregular network digital terrain models," in *SIGGRAPH '79: Procs. of the 6th annual conference on Computer graphics & interactive techniques*, 1979, pp. 199–207.

[10] G. Giralt and L. Boissier, "The french planetary rover vap: Concept and current developments," in *Procs. of the 1992 lEEE/RSJ Int. Conf. on Intelligent Robots and Systems*, vol. 2, 1992, pp. 1391–1398.

[11] E. Krotkov and R. Hoffman, "Terrain mapping for a walking planetary rover," *IEEE Trans. on Robotics & Automation*, vol. 10, no. 6, Dec. 1994.

[12] Y. Kunii, S. Tsuji, and M. Watari, "Accuracy improvement of shadow range finder: Srf for 3d surface measurement," in *Procs. off IEEE/RSJ Int. Conf. on Intelligent Robots and Systems (IROS 2003)*, vol. 3, 27-31 Oct. 2003, pp. 3041 – 3046.

[13] S. Goldberg, M. Maimone, and L. Matthies, "Stereo vision and rover navigation software for planetary exploration," in *IEEE Aerospace Conf. Procs.*, vol. 5, 2002, pp. 2025 – 2036.

[14] S. Laubach and J. Burdick, "An autonomous sensor-based path-planner for planetary microrovers," in *IEEE Int. Conf. on Robotics & Automation*, vol. 1, 10-15 May 1999, pp. 347 – 354.

[15] M. Slack, "Navigation templates: mediating qualitative guidance and quantitative control in mobile robots," *IEEE Trans. on Systems, Man and Cybernetics*, vol. 23, no. 2, pp. 452 – 466, March-April 1993.

[16] L. Yenilmez and H. Temeltas, "Autonomous navigation for planetary exploration by a mobile robot," in *Procs. of Int. Conf. on Recent Advances in Space Technologies (RAST'03)*, 20-22 Nov. 2003, pp. 397– 402.

[17] T. Kubota, R. Ejiri, Y. Kunii, and I. Nakatani, "Autonomous behavior planning scheme for exploration rover," in *Second IEEE Int. Conf. on Space Mission Challenges for Information Technology (SMC-IT 2006)*, 17-20 July 2006, p. 7.

[18] D. M. Gaines, T. Estlin, and C. Chouinard, "Spatial coverage planning and optimization for a planetary exploration rover," in *5th Int. Workshop on Planning and Scheduling for Space*, 2003.

[19] R. Alena, B. Gilbaugh, B. Glass, and S.P.Braham, "Communication system architecture for planetary exploration," *IEEE Aerospace and Electronic Systems Magazine*, vol. 16, no. 11, pp. 4 – 11, Nov. 2001.

[20] C. Lee, R. Alena, T. Stone, J. Ossenfort, E. Walker, and H. Notario, "Software architecture of sensor data distribution in planetary exploration," in *IEEE Aerospace Conf.*, 4-11 March 2006, p. 9.

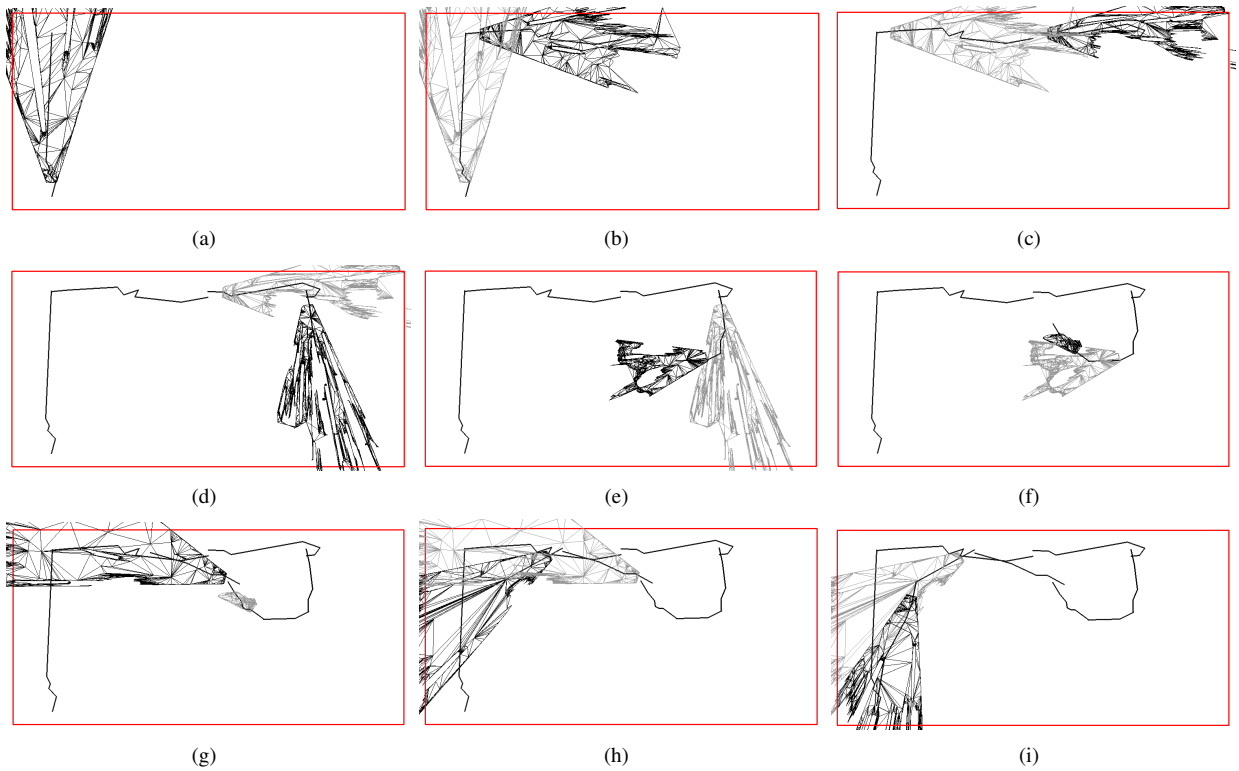

Fig. 9. A sequence of consecutive scans together with the trajectory of the robot. In (a) the first scan is displayed alone, in the next figures (b)-(i) two scans can be seen per image, the latest in black.

[21] J. Wright, A. Trebi-Ollennu, F. Hartman, B. Cooper, S. Maxwell, J. Yen, and J. Morrison, "Terrain modelling for in-situ activity planning and rehearsal for the mars exploration rovers," in *IEEE Int. Conf. on Systems, Man and Cybernetics*, vol. 2, 2005, pp. 1372 – 1377.

[22] A. M. Howard and E. W. Tunstel, Eds., *Intelligence for Space Robotics*. TSI Press, 2006, ch. MER Surface Navigation and Mobility.

[23] F. P. Preparata and M. I. Shamos, *Computational Geometry: An Introduction*. New York, NY: Springer-Verlag, 1985.

[24] "Kitware inc. visualization toolkits." http://www.vtk.org, Website (accessed: September 2005)., 2005.

[25] S. Thrun, W. Burgard, and D. Fox, "A real-time algorithm for mobile robot mapping with applications to multi-robot and 3d mapping," in *In Procs. of the IEEE Int. Conf. on Robotics & Automation (ICRA)*, IEEE, Ed., San Francisco, CA, 2000.

[26] K. Pervölz, A. Nüchter, H. Surmann, and J. Hertzberg, "Automatic reconstruction of colored 3d models," in *Procs. Robotik 2004*, Munich, Germany, u 2004, pp. 215 – 222.

[27] D. Hähnel, W. Burgard, and S. Thrun, "Learning compact 3d models of indoor and outdoor environments with a mobile robot," *Robotics & Autonomous Systems*, vol. 44, no. 1, pp. 15–27, 2003.

[28] P. Allen, I. Stamos, A. Gueorguiev, E. Gold, and P. Blaer, "Avenue: Automated site modeling in urban environments," in *Procs. of the 3rd Conf. on Digital Imaging and Modeling*, 2001, pp. 357–364.

[29] M. Levoy, K. Pulli, B. Curless, S. Rusinkiewicz, D. Koller, L. Pereira, M. Ginzton, S. Anderson, J. Davis, J. Ginsberg, J. Shade, and D. Fulk, "The digital michelangelo project: 3D scanning of large statues," in *Procs. SIGGRAPH*, 2000, pp. 131–144.

[30] A. Davison and N. Kita, "3d simultaneous localisation and map-building using active vision for a robot moving on undulating terrain," in *Procs. IEEE Conf. on Computer Vision and Pattern Recognition*, Kauai, December 2001.

[31] M. Agrawal and K. Konolige, "Real-time localization in outdoor environments using stereo vision and inexpensive gps," in *Int. Conf. on Pattern Recognition (ICPR)*, 2006.

[32] R. Triebel, P. Pfaff, and W. Burgard, "Multi-level surface maps for outdoor terrain mapping and loop closing," in *Procs. of the IEEE/RSJ Int. Conf. on Intelligent Robots and Systems (IROS)*, Beijing, China, 2006, pp. 2276–2282.

[33] É. Dupuis, P. Allard, J. Bakambu, T. Lamarche, and W.-H. Zhu, "Towards autonomous long-range navigation," in *8th ESA Workshop on Advanced Technologies for Robotics & Automation 'ASTRA 2004'*, ESTEC, Noordwijk, The Netherlands, November 2–4 2004.

[34] P. Lamon and R. Siegwart, "Inertial and 3d-odometry fusion in rough terrain towards real 3d navigation," in *IEEE/RSJ Int. Conf. on Intelligent Robots and Systems*, vol. 2, Japan, 2004, pp. 1716 – 1721.

[35] F. Lu and E. Milios, "Globally consistent range scan alignment for environment mapping," *Autonomous Robots*, vol. 4, pp. 333–349, 1997.

[36] M. Montemerlo and S. Thrun, "Simultaneous localization and mapping with unknown data association using fastslam," in *IEEE Int. Conf. on Robotics & Automation*, vol. 2, Taipei, Taiwan, 14-19 Sept. 2003, pp. 1985 – 1991.

[37] K. Lingemann, A. Nüchter, J. Hertzberg, and H. Surmann, "High-speed laser localization for mobile robots," *Journal of Robotics & Autonomous Systems*, vol. 51, no. 4, pp. 275–296, 2005.

[38] A. Nüchter, K. Lingemann, J. Hertzberg, and H. Surmann, "6d slam with approximate data association," in *Procs. of the 12th Int. Conf. on Advanced Robotics (ICAR '05)*, Seattle, Jul. 2005, pp. 242 – 249.

[39] D. Zhang, "Harmonic shape images: A 3d free-form surface representation and its application in surface maching," Ph.D. dissertation, Carnegie Mellon University, 1999.

[40] A. Johnson, "Spin-image: a representation for 3-d surface matching," Ph.D. dissertation, Carnegie Mellon University, 1997.

[41] Y. Sun, J. Paik, A. Koschan, D. Page, and M. Abidi, "Point fingerprint: A new 3-d object representation scheme," *IEEE Trans. on Systems, Man and Cybernetics, Part B*, vol. 33, no. 4, pp. 712–717, 2003.

[42] J. Nsasi Bakambu, S. Gemme, and E. Dupuis, "Rover localization through 3D terrain registration," in *IEEE/RSJ International Conference on Intelligent Robots and Systems*, Beijing, China, 2006.

[43] J. Nsasi Bakambu, P. Allard, and E. Dupuis, "3D reconstruction of environments for planetary rover autonomous navigation," in *Int. Symposium on Robotics*, Tokyo, Japan, 2005.

[44] S. Rusinkiewicz and M. Levoy, "Efficient variants of the ICP algorithm," in *Procs. of the 3rd Intl. Conf. on 3D Digital Imaging and Modeling*, 2001, pp. 145–152.

[45] A. Astolfi, "Exponential stabilization of wheeled mobile robot via discontinuous control," *Journal of Dynamic Systems Measurement and Control*, pp. 121–126, March 1999.

[46] J. N. Bakambu, P. Allard, and E. Dupuis, "3d terrain modeling for rover localization and navigation," in *3rd Canadian Conf. on Computer and Robot Vision (CRV 2006)*, Quebec, June 2006, pp. 61–69.